

Numerical Simulation of Natural Convection of Micropolar Fluid in a Rectangular Porous Enclosure

C Sivarami Reddy, V Ramachandra Prasad, K Jayalakshmi

Abstract: The micropolar fluid in a unsteady free convection of two dimensional rectangular porous enclosure has been examined numerically. The non-dimensional coupled nonlinear partial differential equations is solved by staggered grid based projection method (MAC). The vertical walls of the rectangular enclosure are maintained with different temperatures while both bottom and top walls of the enclosure are considered adiabatic. The heat transfer has been studied for influence of the Rayleigh number (Ra), vortex viscosity parameter (K) and Darcy parameter (Da) on fluid flow. The local Nusselt number reduces with augment of vortex viscosity parameter (K) but it enhances with rise of Darcy number. The results are illustrated in the figures.

Keywords: Porous medium; micropolar fluid; MAC Method; Natural convection; staggered grid.

I. INTRODUCTION

The micropolar fluid theory is induced by Eringen [1] to develop the inadequacy of incompressible Navier-Stokes (N-S) equations to illustrate the right behaviour of different microstructure fluid flows such as muddy water, animal blood, chemical suspensions, colloidal fluids and lubricants [1]. The six degrees of freedom are there in the mathematical theory of micropolar fluids. There are six, out of which three are translation and the remaining are microrotation of microelements. Increasing interest to study convective heat transfer of micropolar flow characteristics because of its several applications in different fields. The detailed micropolar fluid flow theory and its importance can be registered in review articles [2,3] and in the recent book [1,4].

Micropolar fluids filled by Hsu *et al.* [5-7] have examined the thermal convection in enclosures. The help of the method collocation with cubic spline to solve the conservative equations like energy, vorticity, angular momentum, etc. The numerical computation is conducted with influenced value ranges of Gr , Re and wide range values of parameters (material) associated with the microstructure fluid flows (i.e micropolar fluids).

Convective flows through porous media includes wide applications in several fields like science and engineering involving water resources engineering, civil engineering and mechanical, geomechanics, environmental science, bio engineering, material science, petroleum industry etc. They are examined mixed convection heat transfer within enclosure by the influence of vertical moving lids with the bottom hot wall. Basak *et al.* [8] studied combined convection of porous enclosure with motion in vertical lids numerically. [9] reported different thermal wall boundaries of enclosure on convection in a porous enclosure. They are exhibited complex heat flow through Heatline approach for different values of governing key parameters. Sheremet *et al.* [10] with in the porous enclosure the reported finite difference numerical method based study of combined convection of Nano fluid. Their study performed on the effects of solid walls thickness, the thermal conductivity ratio, the thermophoresis parameter, the buoyancy-ratio parameter, the Brownian motion parameter, Lewis numbers and Thermal Rayleigh number on the heat transfer and flow patterns. Natural convection of heat and mass transfer with in a square porous tilted enclosure under the effect of Soret and Dufour have been reported by Chandra Shekar *et al.* [11]. Lattice Boltzmann Method (LBM) based numerical simulation was conducted for convective of nanofluid within a porous enclosure under the effect of non-uniform magnetic field was considered by Sheikholeslami and Shehzad [12]. Thermo-solutal transport phenomena of porous enclosure with triangle shape was examined by Chamkha [13]. Effects of thermal boundary condition of the enclosure wall and also concentration, aspect ratio and angles of inclinations on the flow patterns and temperature contours were analyzed. Finite difference method was adopted to seek the numerical solution. Several researchers have studied convective flows in porous medium for recent years [14-24].

From the above literature review, authors' knowledge the considered in this paper natural convection of micropolar fluid within a rectangular porous enclosure is discussed for the first time. The aim of this article is to analysis of natural convection in a rectangular porous media filled with micropolar fluid. Staggered grid based Marker and Cell Method is select to simulate this paper. Impacts of vortex viscosity parameter, Rayleigh numbers and Darcy number on convective flow in porous enclosure is examined.

Revised Manuscript Received on February 05 2019.

C Sivarami Reddy, Department of Mathematics, JNTU Ananthapur, Anantapuramu 515002, India,

V Ramachandra Prasad, Department of Mathematics, School of Advanced Sciences, Vellore Institute of Technology, Vellore, Tamil Nadu 632014, India,

K Jayalakshmi, Department of Mathematics, JNTU Ananthapur, Anantapuramu 515002, India,



II. MATHEMATICAL FORMULATION

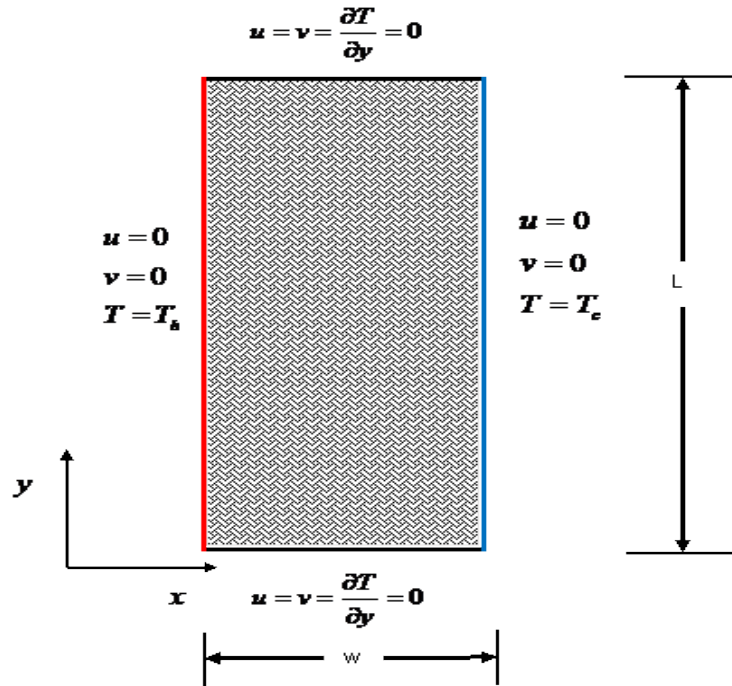


Fig. 1 Physical model and coordinate system

We consider insecure two-dimensional laminar stream of in compressible micropolar fluid of a permeable rectangular nook. The $Y=0$ and $Y=L$ are the two horizontal walls which are thermally insulated when the $X=0$ and $X=W$ of the vertical walls and these are maintained with different temperatures, here length of the enclosure is L and its width is W . The Brinkman extended darcy model, fluid phase for the temperature measurement and solid phase are used in this research work for thermal equilibrium rate conditions.

The cavity left wall is isothermal for boiling temperature T_h and left wall of the enclosure isothermal for cold temperature T_c . The thermo-physical chattels fluid flow is assumed to be constant except fluid density. By applying the Boussinesq approximation, the variation of density results in a body force expressed in momentum equation. Taking into account all the assumptions are mentioned as above, the mass, momentum, angular motion and energy equivalences are represented in the of form dimensional and as follows:

Equation of continuity:

$$\frac{\partial u}{\partial x} + \frac{\partial v}{\partial y} = 0 \quad (1)$$

Momentum:

$$\rho \left(\frac{\partial u}{\partial t} + u \frac{\partial u}{\partial x} + v \frac{\partial u}{\partial y} \right) = -\frac{\partial p}{\partial x} + (\mu + k) \left(\frac{\partial^2 u}{\partial x^2} + \frac{\partial^2 u}{\partial y^2} \right) + k \frac{\partial \eta}{\partial y} - \frac{\mu}{\kappa} u \quad (2)$$

$$\rho \left(\frac{\partial v}{\partial t} + u \frac{\partial v}{\partial x} + v \frac{\partial v}{\partial y} \right) = -\frac{\partial p}{\partial y} + (\mu + k) \left(\frac{\partial^2 v}{\partial x^2} + \frac{\partial^2 v}{\partial y^2} \right) + k \frac{\partial \eta}{\partial x} - \frac{\mu}{\kappa} v + \rho g \beta (T - T_c) \quad (3)$$

Angular momentum:

$$\frac{\partial \eta}{\partial t} + u \frac{\partial \eta}{\partial x} + v \frac{\partial \eta}{\partial y} = \frac{\gamma}{\rho j} \left(\frac{\partial^2 \eta}{\partial x^2} + \frac{\partial^2 \eta}{\partial y^2} \right) - \frac{2k}{\rho j} \eta + \frac{k}{\rho} \left(\frac{\partial v}{\partial x} - \frac{\partial u}{\partial y} \right) \quad (4)$$

Energy:

$$\frac{\partial T}{\partial t} + u \frac{\partial T}{\partial x} + v \frac{\partial T}{\partial y} = \alpha \left(\frac{\partial^2 T}{\partial x^2} + \frac{\partial^2 T}{\partial y^2} \right) \quad (5)$$

$$\text{Where } \gamma = \left(\mu + \frac{k}{2} \right) j,$$

$$t=0 \quad u=v=T=\eta=0 \quad \text{For } 0 \leq x \leq w \quad 0 \leq y \leq l$$

$$t > 0 \quad u = v = 0, \quad \frac{\partial T}{\partial y} = 0 \quad \eta = -n \frac{\partial u}{\partial y} \quad \text{at } y=0, w.$$

$$u = v = 0, T = T_h \quad \eta = -n \frac{\partial v}{\partial x} \quad \text{at } x=0$$

$$u = v = 0, T = T_c \quad \eta = -n \frac{\partial v}{\partial x} \quad \text{at } x=1$$

As the mentioned above mathematical expressions, n referred as constant $0 \leq n \leq 1$. The major case $n=0$ indicates the micro elements strong concentration. Based on that reason illustrates the fluid particle strong concentration, moreover micro-elements of the fluid flow near the walls are

impossible to rotate. The second case, $n=1/2$, consists the diminishes of the stress tensor with anti-symmetric part and also registered a weak concentration. The third case $n=1$ is consists of the modelling of the turbulent part layer flows.

Using the following non-dimensional variables

$$\tau = \frac{t\alpha}{L^2}, (X, Y) = \frac{(x, y)}{L}, U = \frac{uL}{\alpha}, V = \frac{vL}{\alpha}, P = \frac{pL^2}{\rho\alpha^2}, \theta = \frac{T - T_c}{T_h - T_c}, N = \frac{\eta L^2}{\alpha}$$

$$Pr = \frac{\nu}{\alpha}, Ra = \frac{g\beta(T - T_c)L^3 Pr}{\nu^2}, Da = \frac{\kappa}{L^2}$$

$$\frac{\partial U}{\partial X} + \frac{\partial V}{\partial Y} = 0 \quad (6)$$

$$\frac{\partial U}{\partial \tau} + U \frac{\partial U}{\partial X} + V \frac{\partial U}{\partial Y} = -\frac{\partial P}{\partial X} + (1+K)Pr \left(\frac{\partial^2 U}{\partial X^2} + \frac{\partial^2 U}{\partial Y^2} \right) + K.Pr \frac{\partial N}{\partial Y} - \frac{Pr}{Da} U \quad (7)$$

$$\frac{\partial V}{\partial \tau} + U \frac{\partial V}{\partial X} + V \frac{\partial V}{\partial Y} = -\frac{\partial P}{\partial Y} + (1+K)Pr \left(\frac{\partial^2 V}{\partial X^2} + \frac{\partial^2 V}{\partial Y^2} \right) - K.Pr \frac{\partial N}{\partial X} - \frac{Pr}{Da} V + Ra.Pr\theta \quad (8)$$

$$\frac{\partial N}{\partial \tau} + U \frac{\partial N}{\partial X} + V \frac{\partial N}{\partial Y} = \left(1 + \frac{K}{2} \right) Pr \left(\frac{\partial^2 N}{\partial X^2} + \frac{\partial^2 N}{\partial Y^2} \right) - 2K.PrN + K.Pr \left(\frac{\partial V}{\partial X} - \frac{\partial U}{\partial Y} \right) \quad (9)$$

$$\frac{\partial \theta}{\partial \tau} + U \frac{\partial \theta}{\partial X} + V \frac{\partial \theta}{\partial Y} = \frac{\partial^2 \theta}{\partial X^2} + \frac{\partial^2 \theta}{\partial Y^2} \quad (10)$$

With the following wall boundaries are

$$\tau = 0 \quad U = V = \theta = N = 0$$

For $0 \leq Y \leq 1 \quad 0 \leq X \leq 1$

$$\tau > 0 \quad U = V = 0, \quad \frac{\partial \theta}{\partial Y} = 0 \quad N = -n \frac{\partial U}{\partial Y} \quad \text{at } Y=0,$$

L.

$$U = V = 0, \theta = 1 \quad N = -n \frac{\partial V}{\partial X} \quad \text{at } X=0$$

$$U = V = 0, \theta = 0 \quad N = -n \frac{\partial V}{\partial X} \quad \text{at } X=1$$

The stream function ψ evaluated with dimensionless velocity profiles U and V is represented from the motion of flow. The worthy relationship between the velocity components and stream function ψ are

$$U = \frac{\partial \psi}{\partial Y} \quad \text{and} \quad V = -\frac{\partial \psi}{\partial X}$$

The rate of hot wall heat transfer is measured by the below equation

$$Nu = -\frac{\partial \theta}{\partial X} \Big|_{X=0,1}$$

III. SOLUTION OF THE PROBLEM

Present computational problem governing dimensionless nonlinear differential equations (7)-(10) and the corresponding boundary conditions of enclosure walls are solved by numerically. To approximate the convective terms in momentum, angular momentum and conservation energy with the difference scheme of second order accuracy is used. The diffusion terms are approximated using central differences minuet difference scheme. X -momentum and Y -momentum equations are discretized as mentioned above without pressure term then we obtained intermediate velocity profiles. Successive Overrelaxation (SOR) Method is used to find Pressure from Poisson equation while the pressure Poisson equation (PPE).

The final velocity profiles are obtained from the well known method Projection method. Uniform fine grid in the direction of X and Y were considered. For momentum, angular momentum and energy equations then the time integration is terminated when it reaches the steady state explicit time integration is applied.

The steady state was considered to have been reached at when the changes in U , V , θ and N satisfy the equation:

$$\frac{\sum |\zeta^{n+1} - \zeta^n|}{\sum |\zeta^{n+1}|} = 10^{-6}$$

Where ζ stands for velocity, angular velocity and temperature at iteration n .

Code validation

To test the house computational MATLAB code of Marker and Cell (MAC) algorithm with Mahapatra *et al.* [25]. Mahapatra *et al.* [25] reports that the effect of buoyancy ratio on thermosolutal convection of a driven enclosure. The computed results of present house computational code and the results of Mahapatra *et al.* [25] are compared and are presented in Fig 2. This comparison registered worthy agreement for case uniformly heated and uniformly concentrated with $N=50$, $Pr=0.7$ and $Ra=10^3$. Control-volume method and the comparison gives good agreement. This lends confidence into the worthy accuracy of the present numerical code used to get the Mahapatra *et al.* [25] computed numerical results.

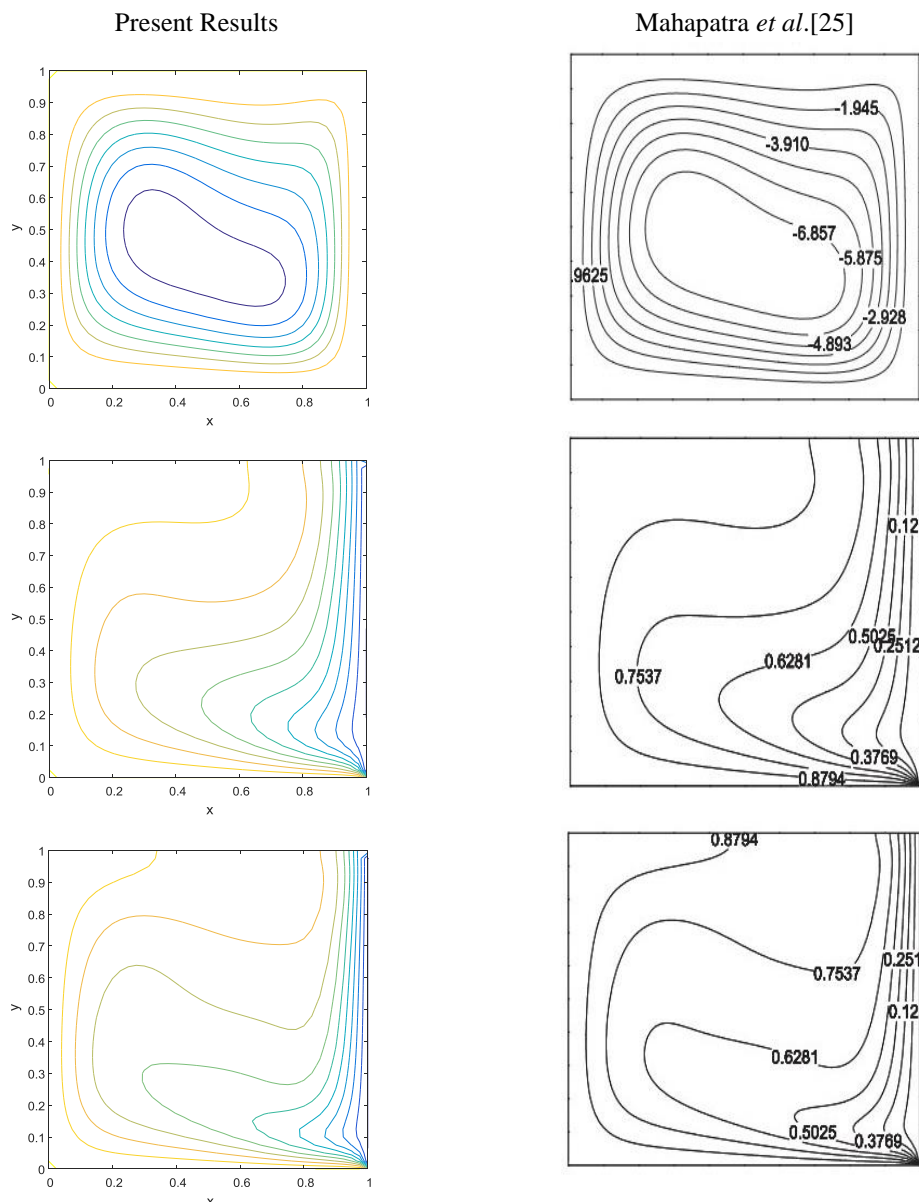


Fig. 2 Comparison of the Streamlines, Isotherms and Isoconcentrations for uniformly heated and uniformly concentrated left and bottom walls with $N=50$, $Pr=0.7$ and $Ra=10^3$

IV. RESULTS AND DISCUSSION

In the present investigation, fluid saturated porous medium with micropolar fluid on opposing temperature gradients have been examined by numerically fills the characteristics fluid particles and temperature distribution due to natural convection in a rectangular cavity. The computation is carried out for wide range of governing

parameters like Rayleigh number ($Ra=10^3-10^6$), Vortex viscosity parameter ($k=0-3$) and Darcy number ($Da=10^{-4}-10^{-1}$). In this computations we consider working fluid Prandtl number take as $Pr=0.71$. The streamline patterns and isotherms distributions and micro-rotation are depicted for various values of governing parameters. The heat flowrate examined hot wall with Nusselt number of local and average respectively.

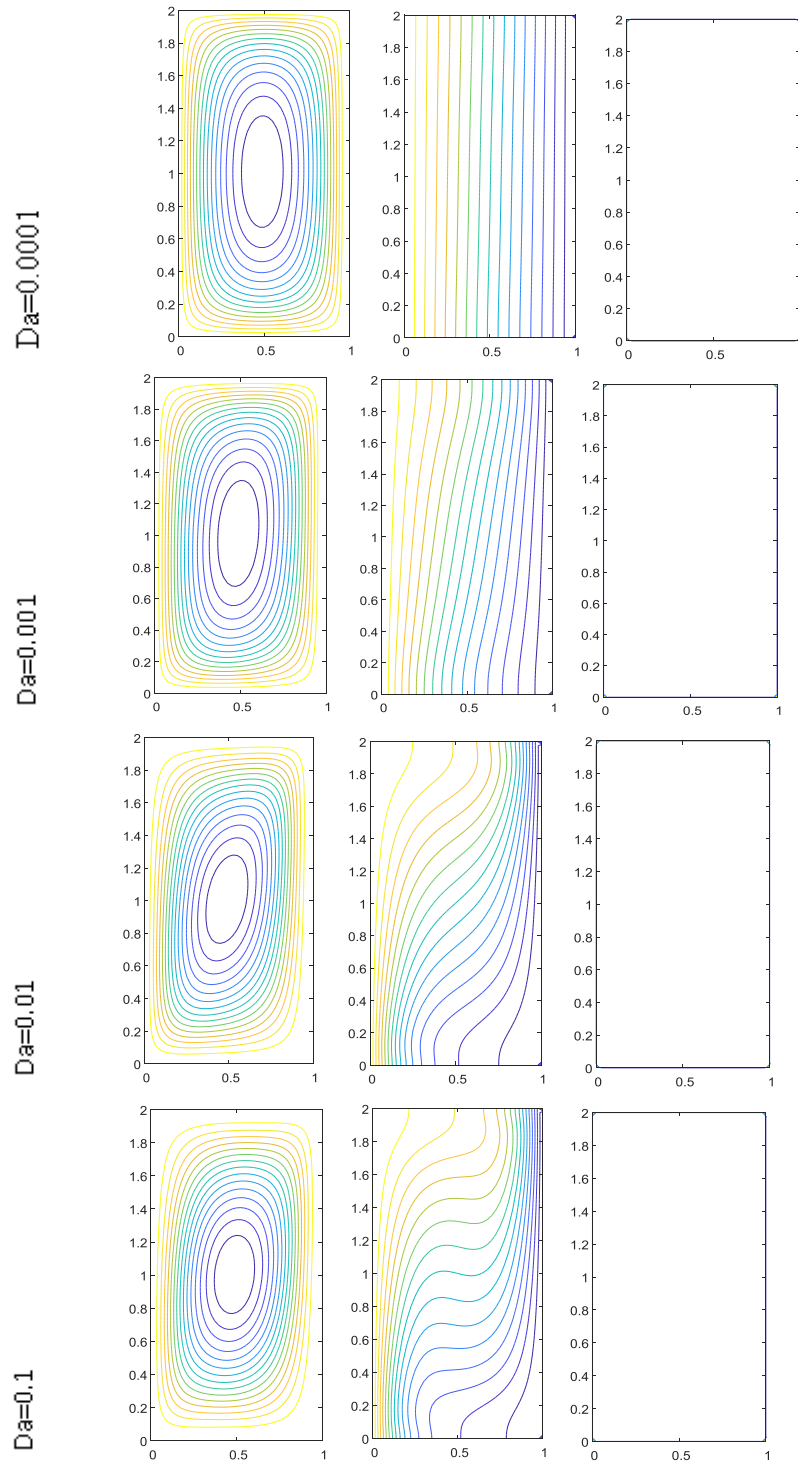


Fig. 3 Steady state patterns of streamlines, isotherms and microrotation for $K=0$, $Pr=0.71$, $Ra=10^4$

Numerical Simulation of Natural Convection of Micropolar Fluid in a Rectangular Porous Enclosure

Fig. 3 shows the isotherms and flow pattern for various values of Da with $Ra=10^4$ and $K=0$. We expect that the fluid flow particles rises up to the down cold wall and falls vertical hot wall. The mechanism generates a mono enlarged vertical elliptical cell with clockwise rotation inside the rectangular enclosure. While, their the corresponding isotherm plots in Fig. 3 it shows that the reduce in the Da

leads to a fall in longitudinal and transverse temperature gradient in the domain due to gradual change in the orientation and the convective forces strength. In tune to the variations of vertical elliptical circulation patterns to clockwise orientation circulation patterns, the temperature readjust the resulting isotherms patterns get vertical to parallel wall of the rectangular enclosure.

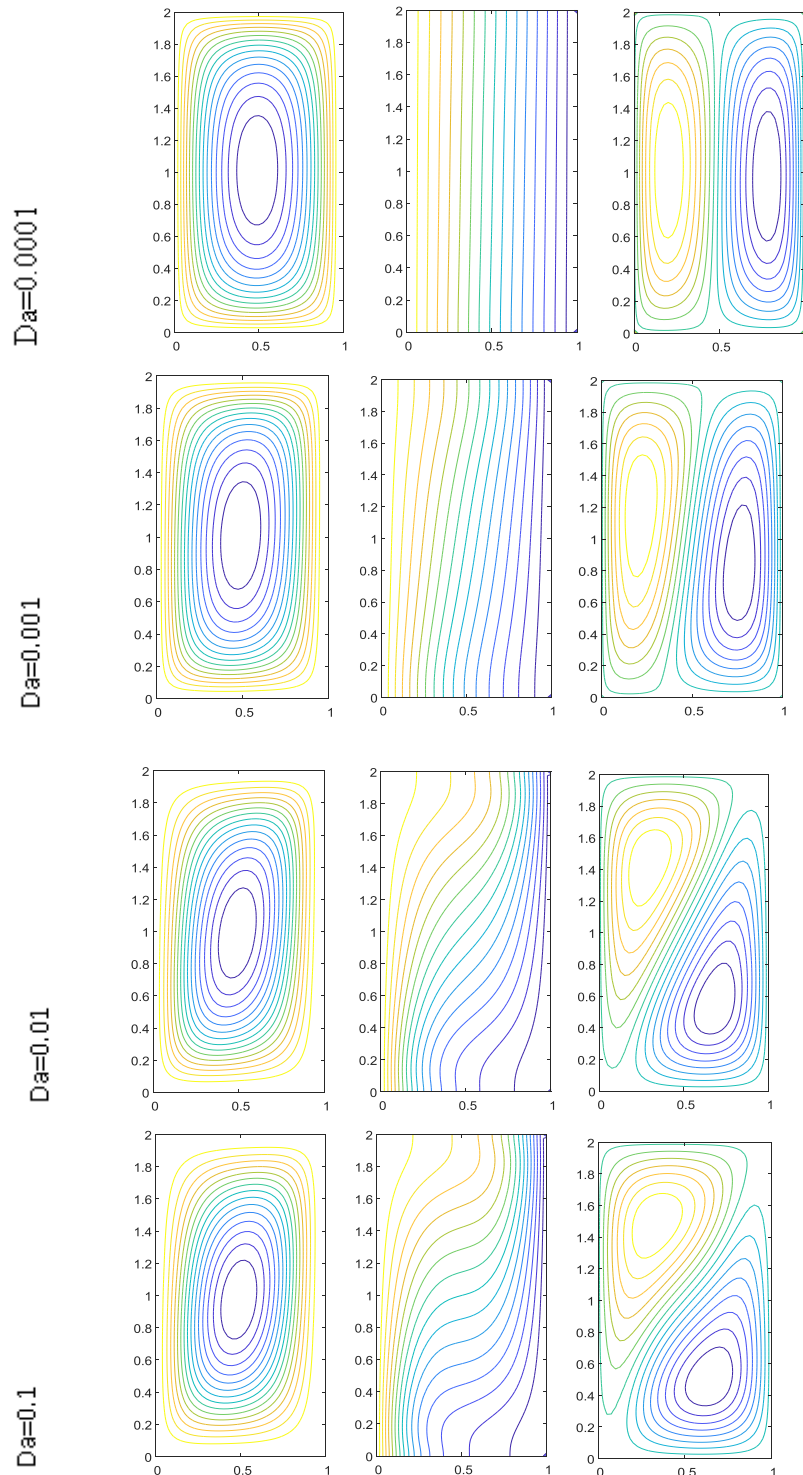


Fig. 4 Steady state patterns of streamlines, isotherms and microrotation for $K=1$, $Pr=0.71$, $Ra=10^4$

Fig. 4 demonstrates the streamlines, isotherms and micro-rotation for various values of Da ($Da=10^{-4}$ - 10^{-1}) with fixed $Ra=10^4$ and $K=1$. From the flow patterns, it is found that a mono enlarged vertical elliptical convective cell is developed inside the rectangular enclosure for low value of $Da=0.0001$. Weaker temperature gradients in entire enclosure due to conduction and isotherms are parallel to the side walls at $Da=0.0001$. Moreover, the Micro-rotation seen that two counter rotating vertical enlarged cells are formed near the side walls of the enclosure at low $Da=0.0001$. Increasing in Darcy number leads to significant changes are noticed in the streamline patterns, isotherms and

micro-rotation. The streamlines reveal the flow patterns within an enclosure for various values of Darcy number. The fluid flow is almost circulated in vertical elliptical shape in all values of Darcy number. The isotherm patterns owe in changing of distribution of temperature contours within the rectangular cavity for varying Darcy parameter. The temperature contours are stretched towards to the cold (top portion) wall and hot wall (bottom portion) with increasing of Darcy parameter Da . Moreover, the micro-rotation is rotates in circular shape in the low temperature portion of the enclosure.

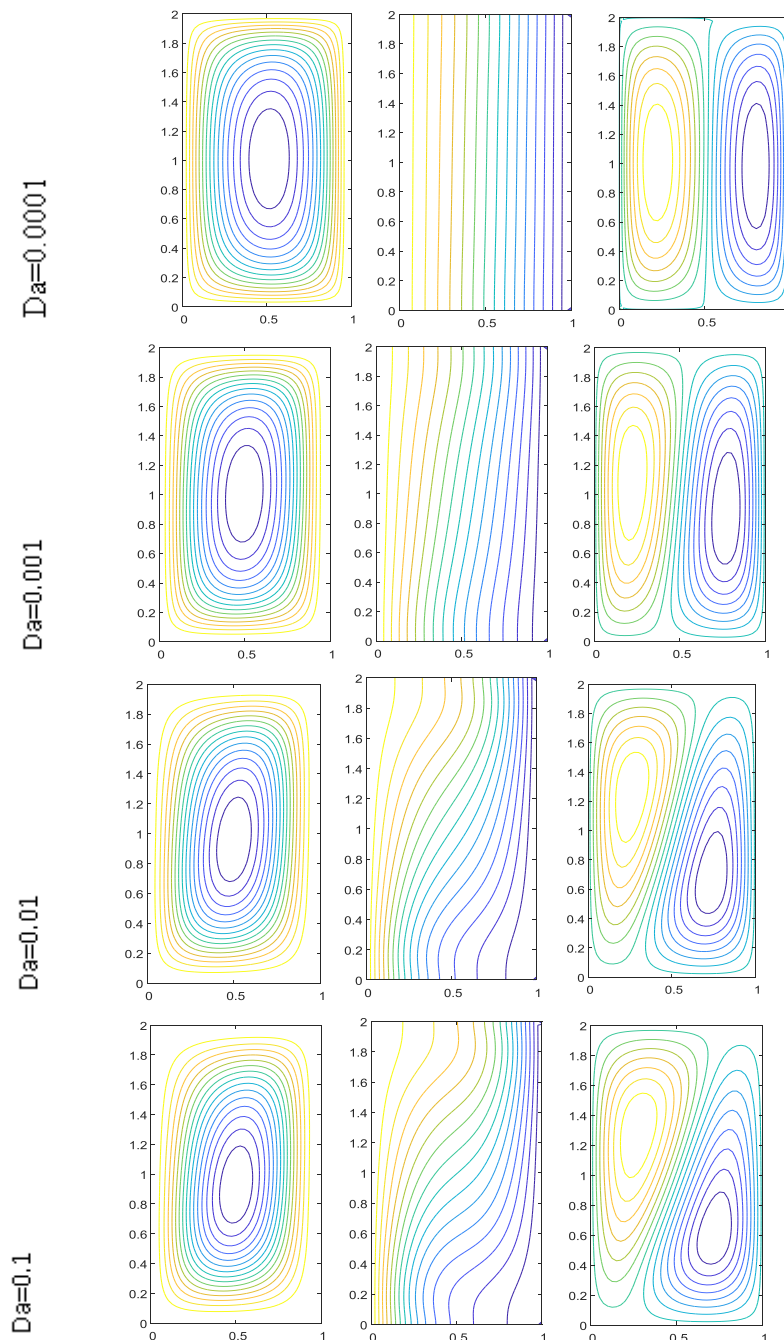


Fig. 5 Stream lines for Steady state patterns, isotherms and microrotation for $K=3$, $Pr=0.71$, $Ra=10^4$

Fig. 5 illustrates the streamlines, isotherms and micro-rotation for different values of Da ($Da=10^{-4}$ - 10^{-1}) with fixed $Ra=10^4$ and $K=3$. Regardless of Darcy number the clockwise vertical elliptical mono enlarged circulation is developed within the enclosure. Notably the regardless of Darcy number two micro-rotation eddies are formed within the boundary but the micro-rotation cells gradually shifted from diagonal elliptical shape to vertically elliptical shape with increasing of Darcy number parameter. The isotherms display different behaviors as Darcy number changes.

For the cases of $Da=0.0001$ and $Da=0.001$, where conduction dominates the flow regime, the temperature contours are occupied whole enclosure tend to be parallel of vertical walls. For increasing of Darcy number Da , the fluid flow become more strengthen and hence the stronger thermal boundary layer developed along the side walls. This is affected the augment of buoyancy force. Moreover, the isotherms are clustered heavily in the top region of the cold wall as well as down region of the hot wall which reveals that the steep temperature gradients arise there.

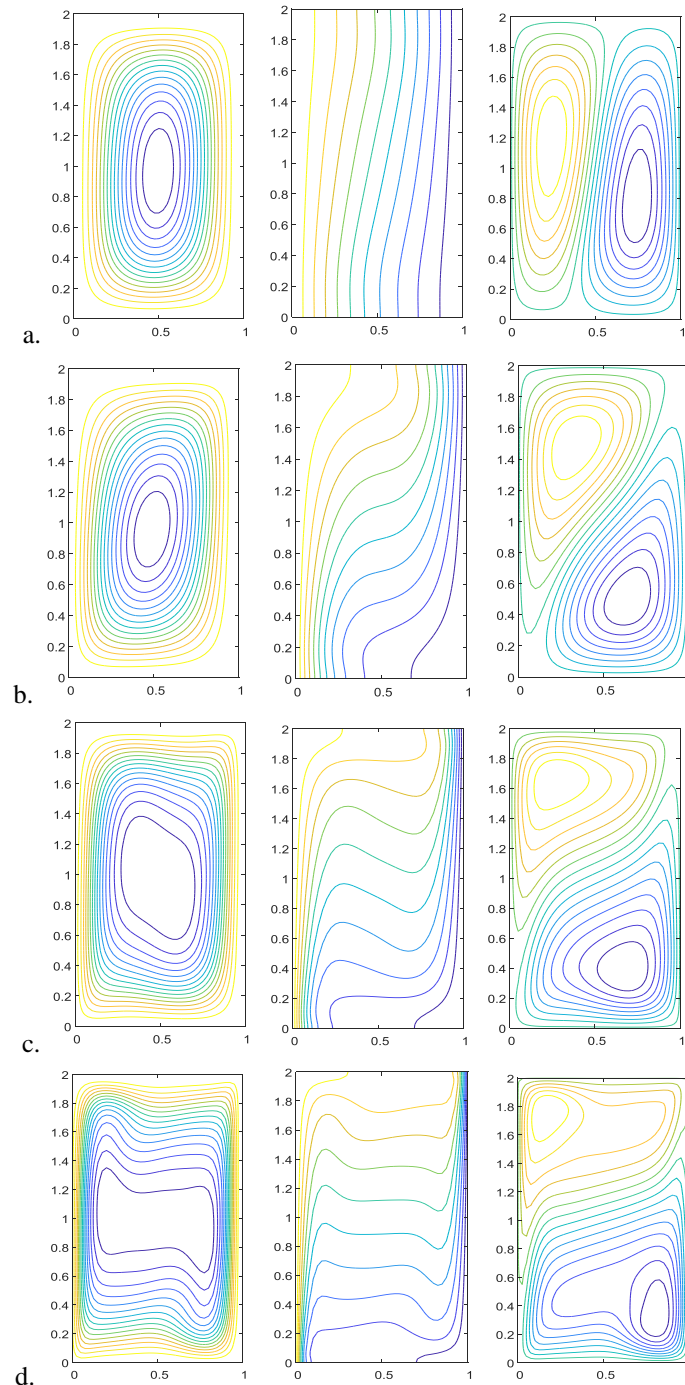


Fig. 6 Steady state patterns of streamlines, isotherms and microrotation for $K=1$, $Pr=0.71$, $Da=0.1$ (a) $Ra=10^3$ (b) $Ra=10^4$ (c) $Ra=10^5$ (d) $Ra=10^6$

Fig.6 consists of The influence of the Rayleigh number on streamlines isotherms and micro-rotations for $k=1$ and $Da=0.1$. We expected, the fluid rises up near the hot wall and descends along the cold wall, which forming a mono enlarged vertical elliptical circulation with clockwise rotation inside the rectangular region. The conduction mechanism is observed for lower Rayleigh number ($Ra=10^3$), which is revealed from the temperature contours. Due to dominant influence of stabilizing the buoyancy effect. When $Ra=10^3$, the elliptic shaped cell is generated at central region, while the Rayleigh number Ra increases its shape changes gradually. The vertical elliptical convective cell is shifted to horizontal when increasing of Rayleigh number Ra from 10^3 - 10^6 which can be seen from the

streamline contour. The clustered isotherms are observed at bottom corner of hot wall and top corner of cold wall except $Ra=10^3$. The steeper thermal gradient increase at side walls with increasing of Rayleigh number Ra from 10^5 - 10^6 while the streamlines are parallel to the horizontal walls in the middle of core regime at $Ra=10^6$. The micro-rotations counts gradually changes registered with increasing of Rayleigh number while the micro-rotation circulations are formed at low temperature regions. The two vertical symmetric micro-rotation circulation are observed at some Rayleigh number $Ra=10^3$ which is caused due to conduction. Moreover, the micro-rotations circulates are moves to cold temperature regions when enhancing of Rayleigh number with in the enclosure.

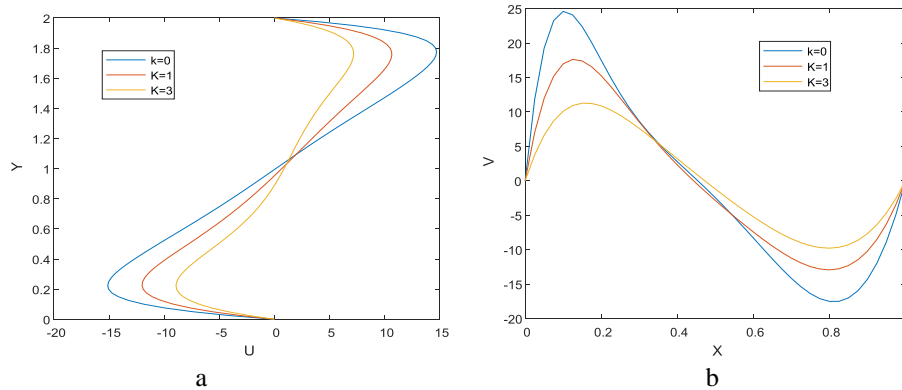


Fig. 7 Central line velocity for $Pr=0.71$, $Ra=10^4$, $Da=0.1$ (a) U -velocity (b) V -velocity

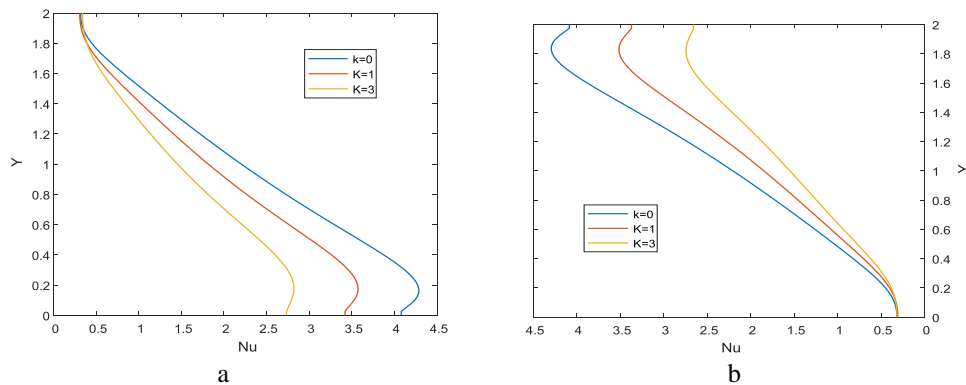


Fig. 8 Local Nusselt number for $Pr=0.71$, $Ra=10^4$, $Da=0.1$ (a) Hot wall (b) cold wall

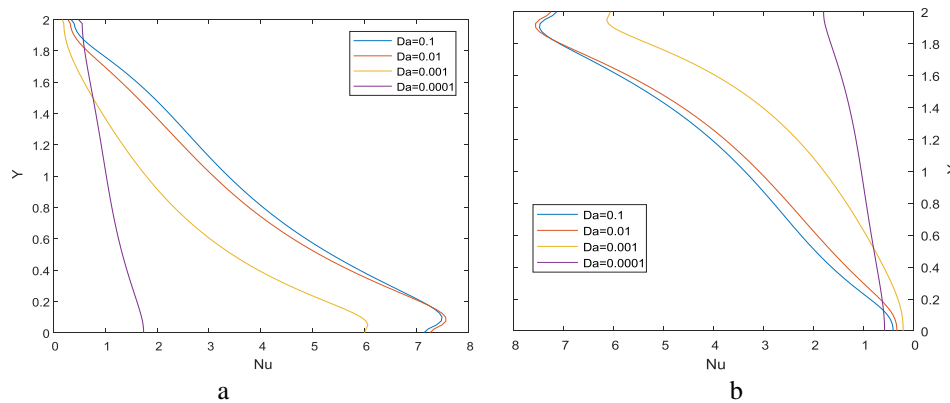


Fig. 9 Local Nusselt number for $K=1$, $Ra=10^5$, $Pr=0.71$ (a) Hot wall (b) cold wall

The variation of mid-section velocity profiles and local Nusselt number for $Pr=0.71$, $Ra=10^4$, $Da=0.1$ with different values of vortex viscosity parameter are shown in Fig. 7 and Fig. 8. It is noticed that the augment of vortex viscosity parameter leads to reduce the mid-section velocity profiles mean while the rate of heat transfer. Moreover, the flow intensity is affected strongly by the vortex viscosity parameter. For various values of Darcy parameter Da for $K=1$, $Ra=10^5$, $Pr=0.71$ is depicted in Fig. 9(a) and Fig. 9(b). The

variation of local Nu_{of} hot and cold walls. For various values of Darcy parameter Da for $K=1$, $Ra=10^5$, $Pr=0.71$ is depicted in Fig. 9(a) and Fig. 9(b). Which describes, the local Nusselt number reduces intensely when increasing in Da from 0.0001 to 0.1. It is interesting to note that the regardless of Darcy number Da local Nusselt number increases more at top portion of the cold wall and the opposite mechanism is exhibited for hot wall.

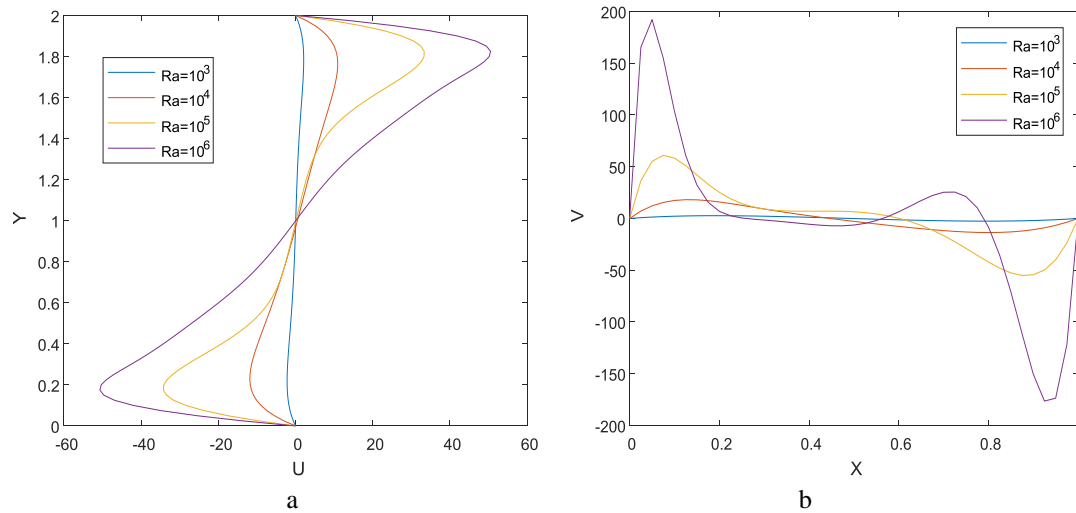


Fig. 10 Central line velocity profiles for $Pr=0.71$, $K=1$, $Da=0.1$ (a) U-velocity (b) V-velocity

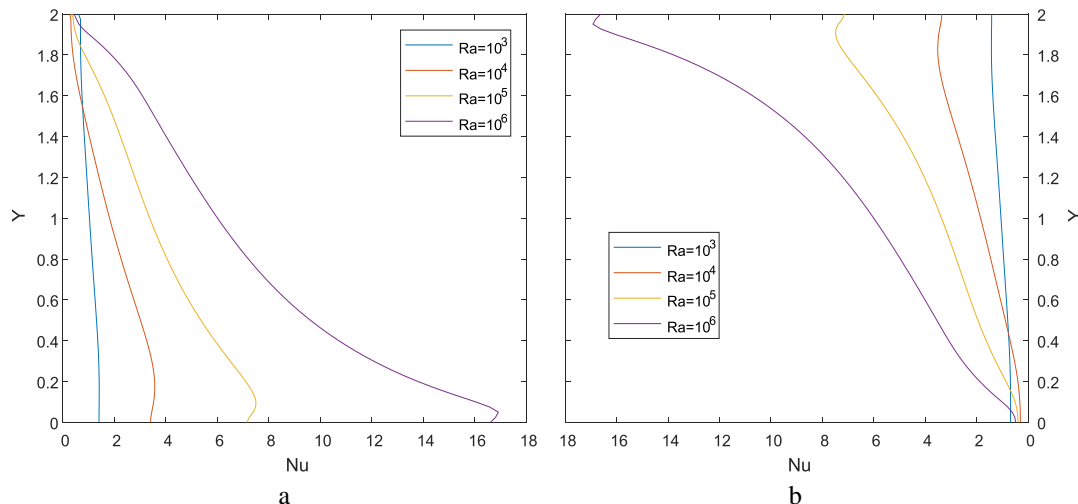


Fig. 11 Local Nusselt number for $Pr=0.71$, $K=1$, $Da=0.1$ (a) Hot wall (b) cold wall

From Fig. 10(a) and (b) illustrate the Central line velocity profiles vertical and horizontal respectively for $Pr=0.71$, $K=1$, $Da=0.1$. for both horizontal and vertical It is observed that raising the Rayleigh number leads to enhancement in midsection velocity. Clearly the buoyancy force not only decelerates the convective velocities but also change its directionality. Fig. 11(a) and (b) exhibits the local Nusselt number of hot and cold walls for various Rayleigh numbers with $Pr=0.71$, $K=1$, $Da=0.1$. the hot and cold wall is increased with an increase of the Rayleigh number for The local Nusselt number. However, the local Nusselt number is increases more at the bottom part of the hot wall and also top portion of the cold wall.

V. CONCLUSION

In this paper, to solve the present investigation partial governing differential equations Projection method based MAC algorithm is used. Convective heat transfer of micropolar fluids in a rectangular enclosure filled with porous medium is studied numerically. The roll of wide range of values of Rayleigh number Ra , vortex viscosity K , Darcy number Da on flow field, the micro-rotation and the rate of heat transfer are discussed through graphically. The following conclusions are obtained.

- The regardless of Rayleigh number, with decreasing in the Darcy parameter, heat transfer rate is suppressed.
- For wide range of K , the augment of Ra the fluid flow rate and temperature distribution are enhanced. While the heat transfers rate and flow rate are reduced when increasing of vortex viscosity parameter K .
- The computed results (isotherms and streamlines) reveal that, vortex viscosity parameter K plays a important role the on enhancement of heat transfer. Higher heat transfer rate is notice when the absence of vortex viscosity parameter K (Newtonian fluid).
- When the vortex viscosity parameter K is increased, a significant reduction in the heat transfer and flow rate is registered for all governing parameters.
- When the Darcy number Da is increased, a significant enhancement in heat transfer and flow rate is registered for all governing parameters.

REFERENCES

1. A.C. Eringen, Microcontinuum Field Theories: II. *Fluent Media*, Springer-Verlag, New York, 2001.
2. T. Ariman, M.A. Turk, N.D. Sylvester, Microcontinuum field mechanics – a review, *International Journal of Engineering Science*, 11 (1973) 905–929.
3. T. Ariman, M.A. Turk, N.D. Sylvester, Applications of microcontinuum field mechanics, *International Journal of Engineering Science*, 12 (1974) 273–291.
4. G. Lukaszewicz, Micropolar Fluids, *Theory and Application*, Birkha'user, Basel, 1999.
5. Hsu, T.-H. and Wang, S.-G., "Mixed convection of micropolar fluids in a cavity", *International Journal of Heat and Mass Transfer*, Vol. 43 (2000) pp. 1563-1572.
6. Hsu, T.H. and Hong, K.Y., "Natural convection of micropolar fluids in an open cavity", *Numerical Heat Transfer, Part A*, Vol. 50 (2006) pp. 281-300.
7. S.K. Jena, L.K. Malla, S.K. Mahapatra, A.J. Chamkha, Transient buoyancy opposed double diffusive convection of micropolar fluids in a square enclosure, *International Journal of Heat and Mass Transfer* 81 (2014) 681–694.
8. Anirban Chattopadhyay, Swapan K Pandit, Sreejata Sen Sarma, I. Pop, Mixed convection in a double lid-driven sinusoidally heated porous cavity, *International Journal of Heat and Mass Transfer* 93 (2016) 361–378.
9. Tanmay Basak, P.V. Krishna Pradeep, S. Roy, I. Pop, Finite element based heatline approach to study mixed convection in a porous square cavity with various wall thermal boundary conditions, *International Journal of Heat and Mass Transfer* 54 (2011) 1706–1727.
10. M.A. Sheremet, I. Pop, Conjugate natural convection in a square porous cavity filled by a nanofluid using Buongiorno's mathematical model, *International Journal of Heat and Mass Transfer* 79 (2014) 137–145.
11. Chandra Shekar Balla, Kishan Naikoti, Soret and Dufour effects on free convective heat and solute transfer in fluid saturated inclined porous cavity, *Engineering Science and Technology, an International Journal* 18 (2015) 543-554.
12. M. Sheikholeslami, S.A. Shehzad, Magnetohydrodynamic nanofluid convective flow in a porous enclosure by means of LBM, *International Journal of Heat and Mass Transfer* 113 (2017) 796–805.
13. Ali J. Chamkha, M. A. Mansour, Sameh E. Ahmed, Double-diffusive natural convection in inclined finned triangular porous enclosures in the presence of heat generation/absorption effects, *Heat Mass Transfer* (2010) 46:757–768.
14. Anwar Bég, O., Prasad, V.R., Vasu, B., Computational modeling of magnetohydrodynamic convection from a rotating cone in orthotropic Darcian porous media, *Journal of the Brazilian Society of Mechanical Sciences and Engineering*, (2017) 39: 2035.
15. Gaffar, S.A., Prasad, V.R. & Reddy, E.K., Computational Study of MHD Free Convection Flow of Non-Newtonian Tangent Hyperbolic Fluid from a Vertical Surface in Porous Media with Hall/Ionslip Currents and Ohmic Dissipation, *International Journal of Applied and Computational Mathematics*, (2017) 3: 859.
16. O. Anwar Bég, S. Abdul Gaffar, V. Ramachandra Prasad, M.J. Uddin, Computational solutions for non-isothermal, nonlinear magnetoconvection in porous media with hall/ionslip currents and ohmic dissipation, *Engineering Science and Technology, an International Journal* 19 (2016) 377–394.
17. A Subba Rao, V Ramachandra Prasad, K Harshavalli, O. Anwar Bég, Thermal radiation effects on non-Newtonian fluid in a variable porosity regime with partial slip, *Journal of Porous Media* 19 (4), 313-329.
18. Debayan Das, Tanmay Basak, Role of discrete heating on the efficient thermal management within porous square and triangular enclosures via heatline approach, *International Journal of Heat and Mass Transfer* 112 (2017) 489–508.
19. Pratibha Biswal, Tanmay Basak, Investigation of natural convection via heatlines for Rayleigh–Bénard heating in porous enclosures with a curved top and bottom walls, *Numerical Heat Transfer, Part A: Applications*, 72:4 (2017) 291-312.
20. Pratibha Biswal, Avijit Nag, Tanmay Basak, Analysis of thermal management during natural convection within porous tilted square cavities via heatline and entropy generation, *International Journal of Mechanical Sciences* 115-116 (2016) 596–615.
21. SVSSNVG Krishna Murthy, BV Kumar, Mohit Nigam, A parallel finite element study of 3D mixed convection in a fluid saturated cubic porous enclosure under injection/suction effect, *Applied Mathematics and Computation* 269 (2015) 841–862.
22. Nikita S Gibanov, Mikhail A Sheremet, Hakan F Oztop, Nidal Abu-Hamdeh, Effect of uniform inclined magnetic field on mixed convection in a lid-driven cavity having a horizontal porous layer saturated with a ferrofluid, *International Journal of Heat and Mass Transfer* 114 (2017) 1086–1097.
23. Mikhail A Sheremet, Cornelia Revnic, Ioan Pop, Free convection in a porous wavy cavity filled with a nanofluid using Buongiorno's mathematical model with thermal dispersion effect, *Applied Mathematics and Computation* 299 (2017) 1–15.
24. MA Sheremet, DS Cimpean, I Pop, Free convection in a partially heated wavy porous cavity filled with a nanofluid under the effects of Brownian diffusion and thermophoresis, *Applied Thermal Engineering* 113 (2017) 413–418.
25. Tapas Ray Mahapatra, Dulal Pal, Sabyasachi Mondal, Effects of buoyancy ratio on double-diffusive natural convection in a lid-driven cavity, *International Journal of Heat and Mass Transfer* 57 (2013) 771–785.